applied sciences

MDPI

Article

Suitability of Active Noise Barriers for Construction Sites

Shahin Sohrabi *, Teresa Pàmies Gómez and Jordi Romeu Garbí

Acoustical and Mechanical Engineering Laboratory (LEAM), Universitat Politècnica de Catalunya (UPC), c/Colom, 11, 08222 Terrassa, Barcelona, Spain; teresa.pamies@upc.edu (T.P.G.); jordi.romeu@upc.edu (J.R.G.)
* Correspondence: shahin.sohrabi@upc.edu; Tel.: +34-93739-8734

Received: 29 July 2020; Accepted: 1 September 2020; Published: 4 September 2020

Abstract: Barriers are increasingly used to protect the pedestrian and neighboring buildings from construction noise activities. This study aims to investigate the suitability of applying active noise control on barriers in a construction site to protect the street area and neighboring buildings. Transducers that are simulated in this work are close to the barrier, and their optimal positions are defined in such a way that the control system has the maximum performance at the neighboring areas close to the construction sites. To begin with, the suitable location of the control sources is found when the total squared pressure is minimized at the positions of noise receivers. The suitable location of the error sensors is, then, found when the control sources are fixed at the position of the previous step and the total squared pressure is minimized at the error sensors. The best location for the error sensors is defined when the maximum reduction is achieved in the target area. It is observed that suitable positions for the transducers depend on the location of target areas for noise control, the position of the noise source, and its operating frequency. In this investigation, a unique configuration is proposed for the transducers that achieves a comparable reduction both at the street area and the neighboring buildings, simultaneously. The results show that the active noise barrier with a height of 2.5 m can achieve an extra insertion loss in the street zone, varies from 9.3 to 16.4 dB (in comparison with passive noise barrier) when the distance of the noise source from the barrier changes in the range of 7 to 1 m, respectively. Those values are of the same order for the passive noise attenuation. Furthermore, similar results are achieved when attempting to cancel the shadow zone of a façade 15 m away from the barrier.

Keywords: noise barrier; active noise control; construction noise control; acoustic protection of façade

1. Introduction

Construction noise is a topic of recognized importance in terms of its impact on workers due to the high noise level generated [1,2]. The issue has gained added significance given the ever-increasing environmental sensitivity of the general public and the corporate sector alike in recent years as construction noise can cause annoyance [3–5] and have adverse behavioral effects [6] on the neighborhood. Among others, the ubiquity of noise sources, the variability of the noise itself, the existence of the flows of materials, people and vehicles, the size of the whole plant, the limited efficiency of most solutions in the low frequency range, and even the difficulty of assessing the effect of mitigating measures [7] all contribute to on-site noise control.

Noise control in this complex scenario generally calls for joint action on the transmitter, using low acoustic emission equipment [8] or managing the schedule and simultaneity of the performances [9], and on the transmission channel [10]. Alternatively, if all else fails, an action can be taken on the receiver [11].

A measure that is gradually being taken is the use of mobile noise barriers that adapt to the construction process [12–15], despite their limited efficiency in the low-frequency range, which predominates in construction noise. The recent study [16] defined the difficulties of the application of active noise barriers in

open space. It is known, however, that active noise control is especially efficient in the low-frequency range, and that is why recent research has focused on applying this strategy to construction noise control, with promising results [9,17]. A natural outgrowth of these recent studies consists of the investigation of the applicability of active noise barriers (ANBs) in construction, which combines portability with maximum efficiency.

Many prior studies also are conducted to predict the behavior of the active noise barrier. Chen et al. [18] investigated the noise reduction mechanisms of active noise barriers. This study shows that at low frequencies, transferred acoustics energy in space is the dominant mechanism when the noise source and control source are well separated. However, the noise reduction mechanism changes to sound absorption and/or radiated energy suppression by the control sources when they are close to the noise source. At high frequencies, the mechanism for noise reduction can be the sound absorption by the control sources. Other studies [19–23] investigated different approaches to control surrounding noise by the active noise barriers. Omoto and Fujiwara [24] evaluated the efficiency of an active noise barrier when error microphones are located on the edge to suppress the diffracted pressure. Their results revealed that reasonable attenuation is achieved when the distance between error microphones on the edge is shorter than half the wavelength of the noise generated by the primary source and when control sources are located to the primary source as close as possible.

Niu et al. [25] carried out an investigation on finding the best position for error microphones near the edge of a noise barrier when 16 control sources were fixed on the top edge. The noise reduction was computed at 6 observational points placed at the shadow zone of the barrier. They conducted theoretical and experimental measurements for three different error microphone placements and their results showed that there is an optimum value between the distance of control sources and error microphones. Their observations showed that when the control sources are located on the top edge of the barrier the best position for the error microphones were placed above the secondary sources. Liu et al. [26] proposed a new arrangement for control sources and error microphones presented in a previously studied case [25]. Their arrangement included two rows with eight units of control sources and corresponded error microphones on the top edge of the barrier. Each row of the control system could work either separately or together. Their results depicted that the maximum attenuation at receivers was attained when both rows of the control system were working simultaneously. Furthermore, they highlighted that the higher the density of secondary sources, the better the control effect.

Hart and Lau [27] examined the performance of an active noise barrier, in which the height of barrier varied from 3 to 5 m, with three control sources and three error microphones linearly arranged above the top edge. The angles of control sources with the barrier changed from 0° to 90°, and the error microphones were always placed perpendicular to the control sources. Their results showed that the angular orientation of the control sources and error microphones is a weak factor for acoustic pressure reduction at the shadow zone when the distance between the control sources and error microphones was less than a quarter wavelength of the primary noise. Chen et al. [28] compared the performance of an active noise barrier with two types of control sources. It is shown that the noise reduction performance of the active noise barrier improves remarkably when the unidirectional control sources were replaced by the monopole control sources. Other investigations [29,30] also show that the efficiency of the active noise barriers depends largely on the number and the location of error microphones and control sources, and the best noise control strategy is canceling the pressure at the target zone. However, real application in a construction site requires a compact design with the transducers located close to the barrier itself so that it can stand as a unique, mobile, and easy to setup device [31,32]. Up to now, only some limited combinations of secondary sources and error microphones deployed around the barrier have been investigated [24,33]. Therefore, there is no knowledge of which is the best possible configuration for a certain application, as, e.g., noise from construction activities.

This study sets out to investigate the suitability of applying active noise control on barriers for construction sites and defining the configuration of the control devices, which gives the maximum attenuation. The suitable locations for the transducers are found among 341 potential positions around

the barrier. The cancelation targets for noise control are the neighboring street area, defined by a horizontal plane of receivers at the shadow zone of the barrier, and buildings close to the construction site, defined by a vertical plane of receivers' places away from the barrier.

In this regard, two stages are involved in discovering the best location of the transducers close to the barrier [34–39]: First, the position of the control sources is found ensuring the maximum attenuation of acoustic pressure in the receiver zone. Second, a suitable position is selected for the error microphones that gives the greatest attenuation in the shadow area for the location of the control sources found in the first stage.

2. Theory

2.1. Diffraction Model

Numerous available methods estimate the diffracted sound field. An analytical model is preferable in the case of a repetitive calculation due to its low computational requirements. Among the various analytical models proposed for calculating the pressure of diffracted sound wave, the one developed by MacDonald [40] is widely used for the barrier calculations, which we have also used throughout this study.

Given one receiver, one sound source, and one semi-infinite barrier, three different acoustic fields are found depending on the relative locations of these elements [30]. These fields include the shadow zone of the barrier (Region I), Region II, and Region III as shown in Figure 1.

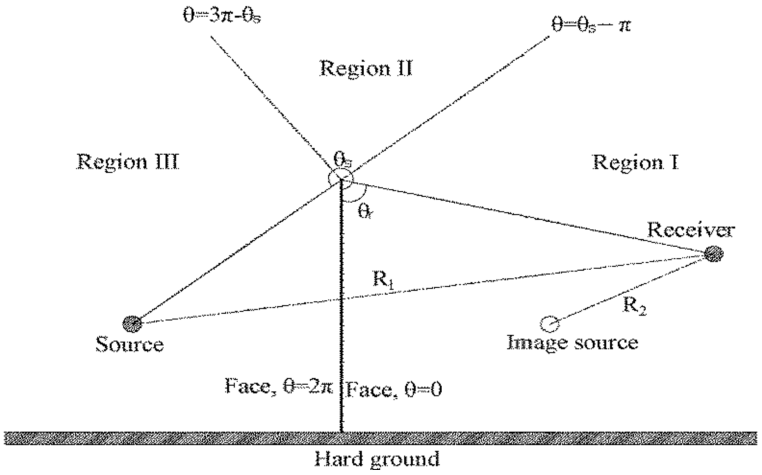

Figure 1. Schematic diagram of the diffraction wave [30].

The receivers in the incident zone (Region III) are in the direct, reflected, and diffracted field of the sound source. However, the barrier reflected wave fronts disappear in Region II, and only diffracted field remains in the Region I.

Equation (1) represents the MacDonald's solution for computing the pressure of diffracted wave fronts along the barrier edge.

$$P_D = \frac{k^2 \rho\, c}{4\pi} q_0 [sgn(\zeta_1) \int_{|\zeta_1|}^{\infty} \frac{H_1^{(1)}\left(kR_1 + s^2\right)}{\sqrt{s^2 + 2kR_1}}\, ds + sgn(\zeta_2) \int_{|\zeta_2|}^{\infty} \frac{H_1^{(1)}\left(kR_2 + s^2\right)}{\sqrt{s^2 + 2kR_2}} ds] \quad (1)$$

where k is the wave number, q_0 ($m^3\ s^{-1}$) is the source strength, and ρ and c are the air density and the sound speed, respectively. $H_1^{(1)}(\ )$ is the Hankel function of the first kind, R_1 and R_2 are the distances from the source and its barrier image to the receiver, respectively, as illustrated in Figure 1. In this

regard, s is the variable of the contour integral and the limits of the two contour integrals in Equation (1) are determined according to:

$$\zeta_1 = \mathrm{sgn}(|\theta_s - \theta_r| - \pi)\sqrt{k(R' - R_1)} \tag{2}$$

$$\zeta_2 = \mathrm{sgn}(\theta_s + \theta_r - \pi)\sqrt{k(R' - R_2)} \tag{3}$$

where $\mathrm{sgn}()$ is the sign function, and θ_s and θ_r are the source and receiver angles, respectively. R' is the shortest path from the source to the receiver through the edge. Keeping in mind that all the sources are considered as three-dimensional point sources, they create direct and reflection acoustic pressure as follows,

$$P_d = \frac{-ik\rho\, c}{4\pi} q_0 \frac{e^{ikR_1}}{R_1} \tag{4}$$

$$P_r = \frac{-ik\rho\, c}{4\pi} q_0 \frac{e^{ikR_2}}{R_2} \tag{5}$$

2.2. Active Noise Barriers

The overall objective of adding active noise control sources to the barriers is to extend the efficiency of the acoustic barriers at low-frequency spectra, typical of construction noise [8]. An effective design of an active noise barrier defines the location of the error microphones and secondary sources properly. Installing the transducers close to the barrier can be advantageous in terms of supporting them on the barrier itself. The optimized position of transducers highly depends on the position of the noise source and the target area where it is aimed to control the sound level.

In this study, the locations of transducers are optimized for different positions of the noise sources and two different target areas, namely, the street area and the façade of the neighboring building. The optimization procedure is followed by a two-step method [34–39]. The first step is to determine the positions of the control sources, which ensures the maximum noise level reduction in the target area. Once the suitable location of the control source has been found, the position of the error microphones is defined. It bears noting that the objective in the second step is not to maximize the attenuation in the error sensors, but to minimize the sound level in the target area.

Minimization of Squared Pressure

The total pressure at the discrete number of points described by $\boldsymbol{P}$, can be written in terms of the primary's and secondary sources' strengths in the form of

$$\boldsymbol{P} = \boldsymbol{Z}_P q_P + \boldsymbol{Z}_s \boldsymbol{q}_s \tag{6}$$

where $\boldsymbol{Z}_P$ is the vector for complex acoustic transfer impedances for the primary source at these points and q_P is the primary source strength. $\boldsymbol{Z}_s$ is an $M \times N$ impedance matrix, corresponding to N control sources at M points, and $\boldsymbol{q}_s$ is the vector for the control source's strength.

Equation (7) defines the total squared pressure

$$\boldsymbol{J}_p = \boldsymbol{P}^{\boldsymbol{H}}\boldsymbol{P} = \boldsymbol{Z}_P^H \boldsymbol{Z}_P + \boldsymbol{Z}_P^H \boldsymbol{Z}_s \boldsymbol{q}_s + \boldsymbol{q}_s^H \boldsymbol{Z}_s^H \boldsymbol{Z}_p + \boldsymbol{q}_s^H \boldsymbol{Z}_s^H \boldsymbol{Z}_s \boldsymbol{q}_s \tag{7}$$

The strength of control sources is computed by minimizing the total squared pressure. The unique minimum value is specified by [41]

$$\boldsymbol{q}_s = -\left(\boldsymbol{Z}_s^H \boldsymbol{Z}_s\right)^{-1}\left(\boldsymbol{Z}_s^H \boldsymbol{Z}_p\right) \tag{8}$$

Then, regarding broadband spectra, Equation (9) calculates the overall insertion loss, $\overline{IL}$, at all observational points in the target area through all frequencies in the desired range.

$$\overline{IL} = 10\, log(\frac{\sum_{i=1}^{i=13}\sum_{j=1}^{j=M}\left|P_{ij}^{OFF}\right|^2}{\sum_{i=1}^{i=13}\sum_{j=1}^{j=M}\left|P_{ij}^{ON}\right|^2}) \quad (9)$$

where $P_{ij}^{ON} = \boldsymbol{Z}_P q_P + \boldsymbol{Z}_s \boldsymbol{q}_s$ and $P_{ij}^{OFF} = \boldsymbol{Z}_P q_P$ are the total pressures in the target area with and without control, respectively. In this study, i refers to the central frequency of the third of the octave band between 63 Hz and 1 kHz, at any j position of the observational points.

3. Method

Acoustic barriers are commonly used in cities to control the construction noises in the street area and neighboring buildings. These kinds of barriers are generally composed of several short length segments (Figure 2) so that they can be installed, moved, and adapted to the boundary of the construction sites. In this study, three zones are considered to model the construction site and its nearby areas: (I) the construction site (Figure 2a), where the activities are progressing and the noise sources are located; (II) the building area, representing close buildings; and (III) the street area, representing the sidewalk zone between neighborhood buildings and the construction site (Figure 2b).

(**a**) (**b**)

Figure 2. On-site noise control barriers. (**a**) Construction site area. (**b**) Sidewalk and neighboring buildings.

In the simulation, the barrier with rigid surfaces on both sides and a practical height of H_b = 2.5 m is considered between the construction site and the sidewalk and buildings area (Figure 3). The thickness of the barrier is considered negligible vis-a-vis the noise wavelength. In the calculations, the ground is also assumed to be hard and the reflected pressure at both sides of the barrier are computed based on the image method [42].

To address the movement of the noise source in the construction site, the simulation is conducted for different positions of the noise source. The distance of the noise source from the barrier, d_{pr}, ranges from 1 to 7 m, and for simplicity, it is always located at plane Y = 0 and a height of 0.3 m. The frequency spectra throughout this work are formed by the center frequency of each third octave band from 63 Hz to 1 kHz and the power output of the noise source is 1 W at each considered frequency.

Figure 3 schematically shows the construction site and the nearby areas. In this figure, the control zone is the region close to the barrier, reserved to place the transducers. This zone is intentionally selected near the barrier so that the transducers can be installed in real applications and also the active barrier remains as a unique, portable device. For this study, the control zone surrounds the barrier with a size of 1×3 m^2.

The positions of the transducers are optimized through the control zone to minimize the sound level in the target areas (shaded areas in Figure 3). The street area with a size of 10×8 m^2 is recognized

as the first target area that is covered with 15 points for computing the pressure. These points are located at a height of 1.65 m.

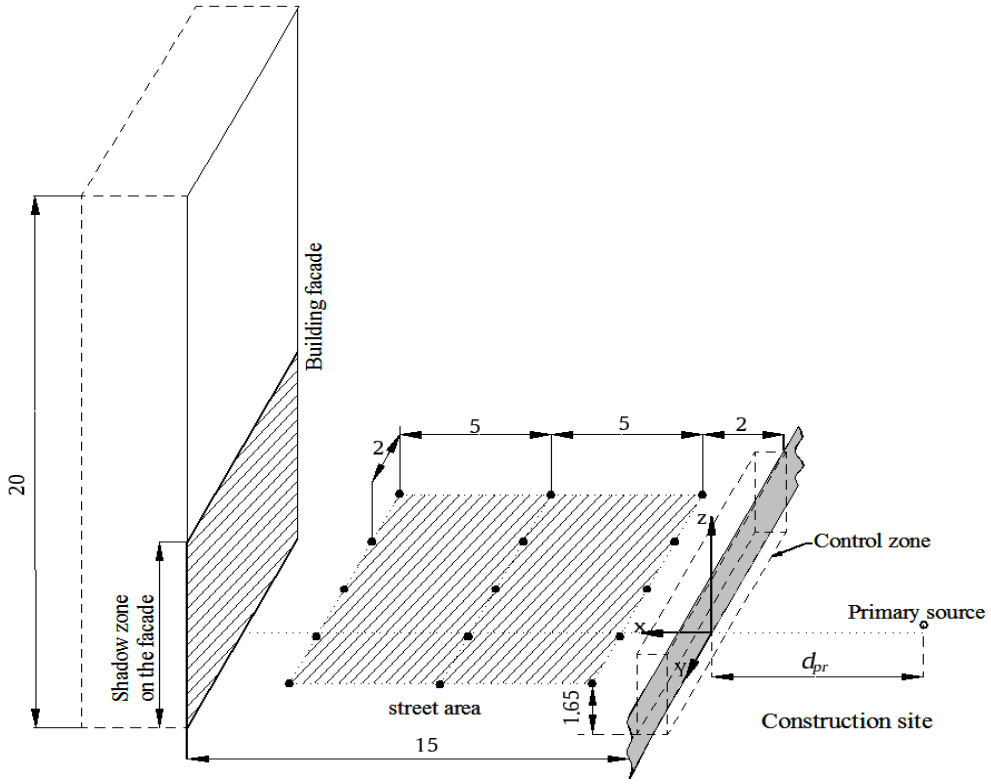

Figure 3. Schematic diagram of an infinite barrier and different target zones (dimensions are in meter).

The second target area in this research is the shadow zone on the façade of the neighboring building. The whole building façade is 20×8 m^2, located on the plane $X = 15$ m (Figure 3) and placed symmetrically with respect to the Y-axis. The size of the shadow zone on the façade depends on the relative location of the noise source from the barrier. In the current work, the same density of points as the street area is always considered to compute the pressure on the façade.

The set of control sources is defined by an array of $N_s = 10$ control sources arranged linearly along the Y-direction and distributed symmetrically with respect to the X-axis. The space between the adjacent control sources in the Y-direction is $d_s = 0.2$ m, which is close to half the shortest wavelength at 1 kHz, a distance that gives a better performance for an array of control sources [24,43]. The suitable location for the control sources is found among 341 candidate positions in the control zone (Figure 3), defined by a grid of 0.1 m steps in both X- and Z-direction. For each candidate position, the strength of the control sources is calculated so that the acoustic pressure is minimized at the observational points in the target areas, calculated using Equation (9). The position that gives the maximum attenuation is considered as the best location for the control sources.

Once the best location of the secondary sources has been defined, minimizing the acoustic pressure level in the target areas is attempted using a set of error sensors within the control zone. To this end, an array of $N_e = 41$ error microphones is arranged linearly along the Y-direction, with distances $d_e = 0.2$ m between them, and distributed symmetrically with respect to the X-axis. The distance between error sensors is close to half the shortest wavelength which, based on ref. [24,43], is the optimum value for the separation space of error sensors, and $N_e = 41$ is chosen to cover the width of the target areas in Y-direction. With the secondary sources fixed at the best position of each frequency, the strength of the control sources is calculated to minimize the squared pressure at the error microphones in all candidate positions in the control zone. The position that, after the previous

calculation, gives the maximum attenuation in the target area, calculated by Equation (9), should provide the best setup of the control sources and error microphones within the control zone.

4. Results

This section introduces the best locations of the transducers in the control zone when different regions are considered as the target zones.

4.1. Target Area: Street Area

Table 1 shows the position of transducers, which gives maximum attenuation in the street area for the various distances of the noise source from the barrier (d_{pr}). This table also illustrates the different values of attenuations reached in the street area ($\overline{IL}_s$), the shadow zone on the façade ($\overline{IL}_{F.s}$), and at the whole building façade ($\overline{IL}_F$), considering passive and active noise control mechanisms.

Table 1. Best positions for the transducers and the insertion loss achieved when the street area is the target zone. d_{pr} is the distance of the noise source from the barrier and $\overline{IL}_s$, $\overline{IL}_{F.s}$, and $\overline{IL}_F$ are the average insertion loss in the street area, in the shadow zone of the façade, and in the whole building, respectively. The insertion loss with the passive noise barrier (PNB), is the difference of the average sound pressure level in the observational points with and without barrier, and the insertion loss of the active noise barrier (ANB) is computed by Equation (9). (X_s, Z_s), (X_e, Z_e) are the coordinates of the control sources and error sensors, respectively.

d_{pr} (m)	(X_s, Z_s) (m)	(X_e, Z_e) (m)	$\overline{IL}_s$ (dB)		$\overline{IL}_{F.s}$ (dB)		$\overline{IL}_F$ (dB)	
			ANB	PNB	ANB	PNB	ANB	PNB
1	(−0.5, 0)	(0.5,2.4)	16.4	14.9	17.9	10.8	17.9	10.8
2.5	(−0.5,1.8)	(0.5,1.1)	11.9	13.2	10.8	9.6	0.9	8.7
4	(−0.5, 1.8)	(0.5,0.9)	10.9	12.3	8.4	9.5	−0.3	8.3
5.5	(−0.5, 1.8)	(0.4,0.4)	9.9	11.8	8.1	9.2	−0.4	8.3
7	(−0.5, 1.8)	(0.4,0.2)	9.3	11.4	7.9	9.1	−0.1	8.3

This table shows that the best position of the transducers varies depending on the location of the noise source. As changing the position of the transducers according to the distance between the noise source and the barrier is not a practical solution, it is worth to seek whether there are regions in the control zone for the control devices where the active noise control can achieve comparable attenuations for different locations of the noise source. Figure 4-i shows the reduction in the street area ($\overline{IL}_s$) achieved from the first step for different positions of the control sources in the control zone. The location of the noise source changes from d_{pr} = 1 m (Figure 4a-i) to d_{pr} = 7 m (Figure 4e-i). In this figure, the barrier is shown by a black bar and * represents the best position of the control sources.

Form the second step, Figure 4-ii illustrates the reduction in the street area ($\overline{IL}_s$) when the control sources are located in the best position (the star position) and the total square pressure is minimized in different positions of the error sensors in the control zone. In Figure 4-ii, ■ is the most suitable position for the error microphones.

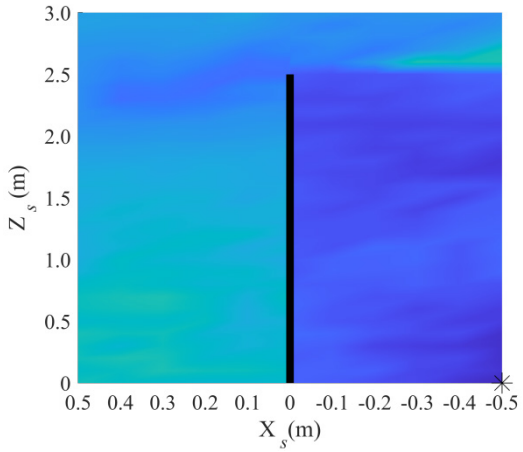

(a-i)

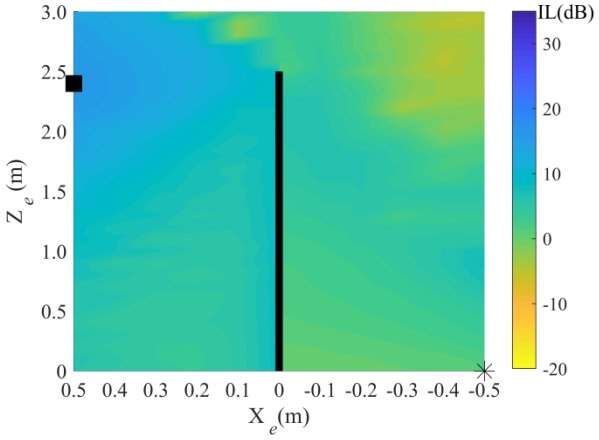

(a-ii)

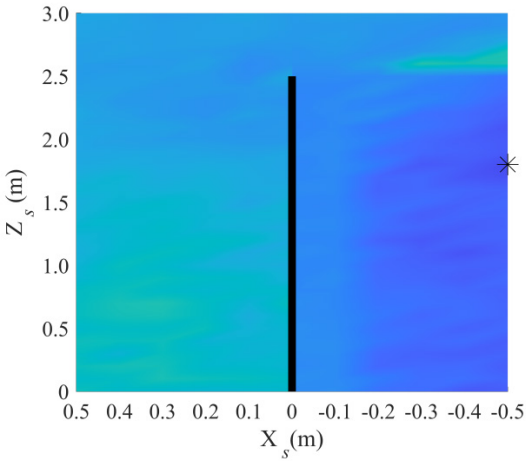

(b-i)

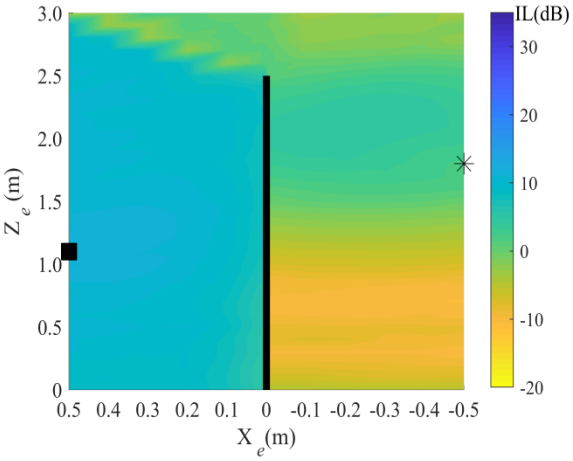

(b-ii)

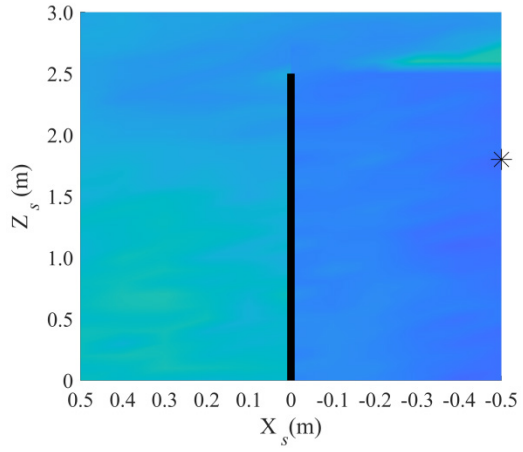

(c-i)

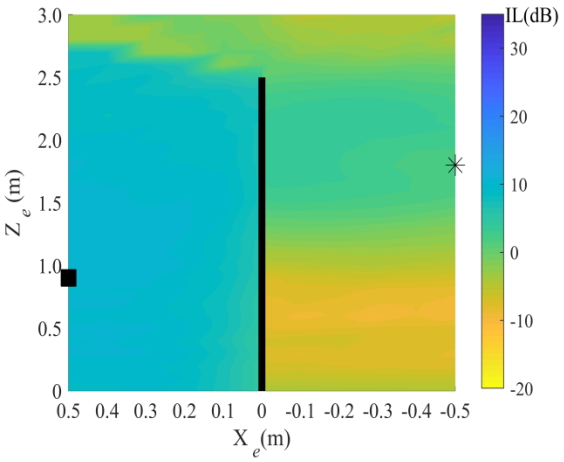

(c-ii)

Figure 4. *Cont.*

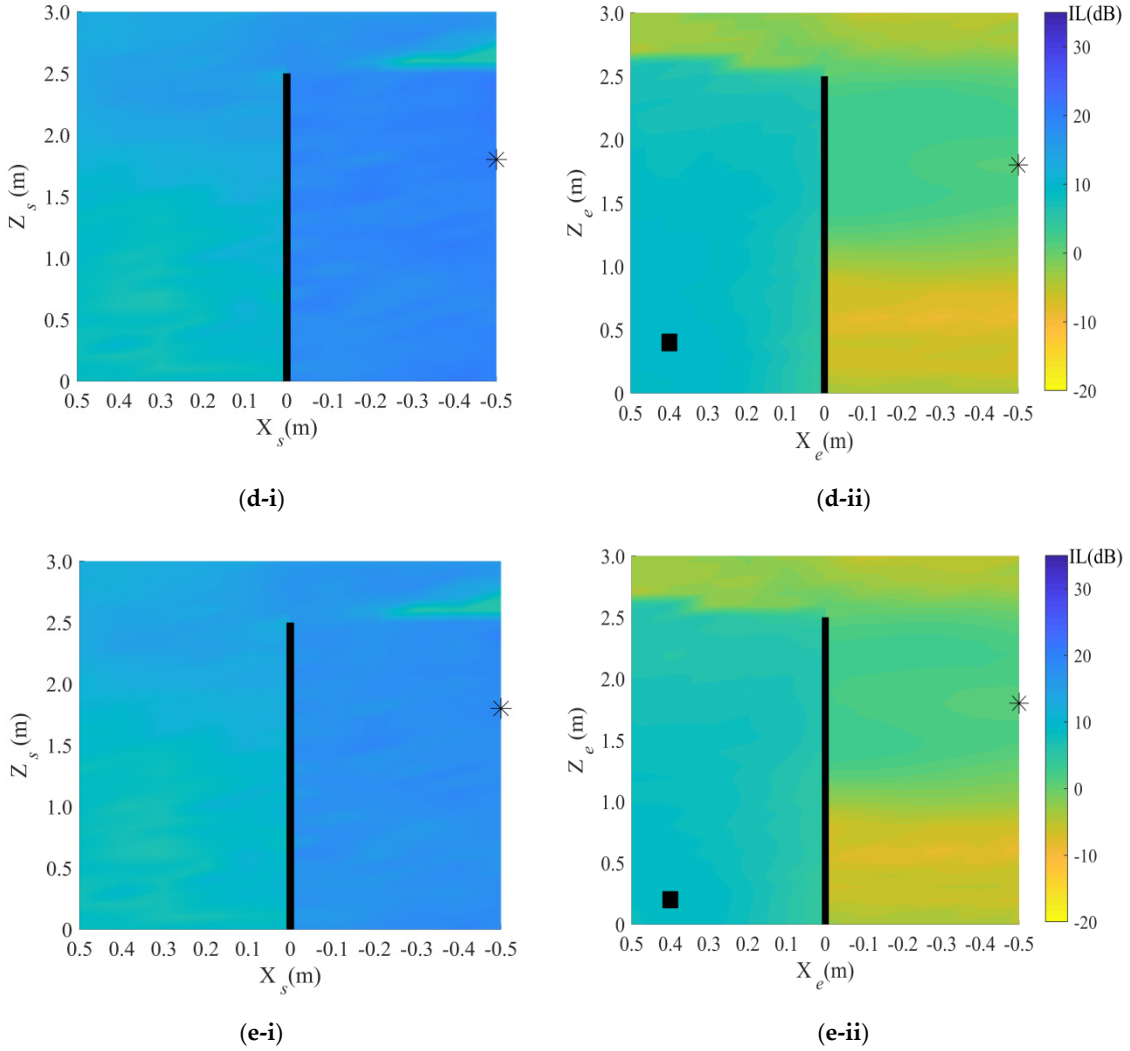

Figure 4. $\overline{IL_s}$ (dB) for different positions of (**i**) secondary sources and (**ii**) error microphones, in the control zone. The distance of the noise source from the barrier (d_{pr}) is (**a**): 1 m, (**b**) 2.5 m, (**c**) 4 m, (**d**) 5.5 m, and (**e**) 7 m. The barrier is presented by the black bar, and * and ■ represent the best positions of the control sources and error microphones, respectively.

4.2. Target Area: Shadow Zone of the Façade

More studies have simulated the effect of noise cancelation by the barrier on the façade of a tall building nearby a construction site. In this subsection, the shadow zone on the façade is considered as the target area to control the noise of construction activities. The height of the shadow zone on the façade depends on the distance of the barrier to the building and the distance of the noise source from the barrier (d_{pr}). In this study, the height of the shadow zone on the façade changes from 7 m for the noise source at d_{pr} = 7 m to the whole façade for d_{pr} = 1 m. Table 2 demonstrates the most suitable configurations of the transducers when the shadow zone of the façade is considered as the control target area.

Figure 5 illustrates the average reduction in the shadow zone on the façade ($\overline{IL_{F,s}}$) for different positions of the secondary sources and error sensors described in Figure 4. In this figure, the target area is the shadow zone on the façade.

Table 2. The best positions of the secondary sources and error microphones in the control zone, when the target zone is the shadow zone of the façade. Variables are similar to Table 1.

d_{pr} (m)	(X_s, Z_s) (m)	(X_e, Z_e) (m)	$\overline{IL_s}$ (dB)		$\overline{IL_{F.s}}$ (dB)		$\overline{IL_F}$ (dB)	
			ANB	PNB	ANB	PNB	ANB	PNB
1	(−0.5, 0)	(0.2, 2.3)	11.8	14.9	22.0	10.8	22.0	10.8
2.5	(−0.5,1.9)	(0.5, 0.5)	11.4	13.2	12.1	9.6	0.6	8.7
4	(−0.5,1.8)	(0.3, 0.3)	10.3	12.3	9.7	9.5	−0.5	8.3
5.5	(−0.5,2.3)	(0.5, 0.2)	10.7	11.8	9.4	9.2	1.1	8.3
7	(−0.5,2.3)	(0.3,0.4)	8.3	11.4	8.9	9.1	0.1	8.3

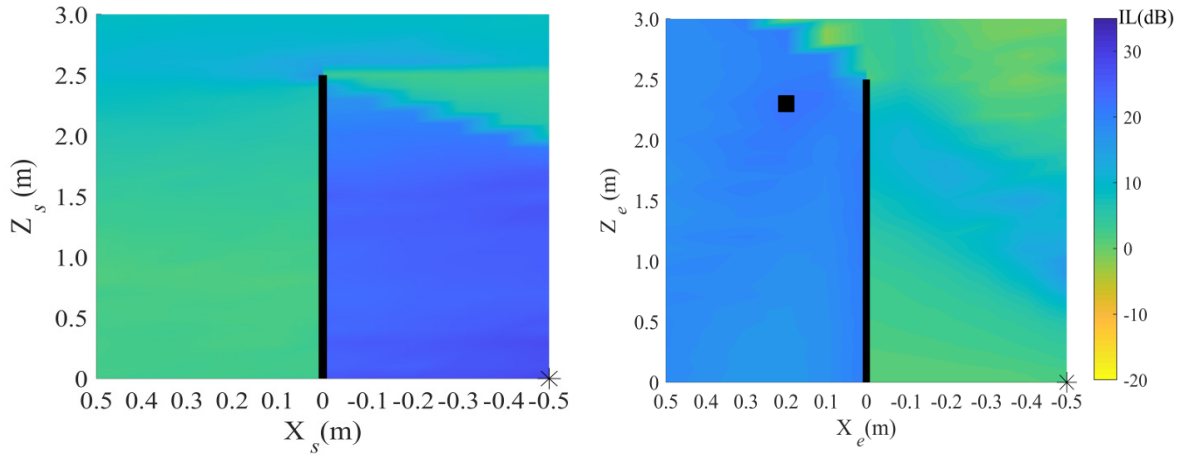

(**a-i**) (**a-ii**)

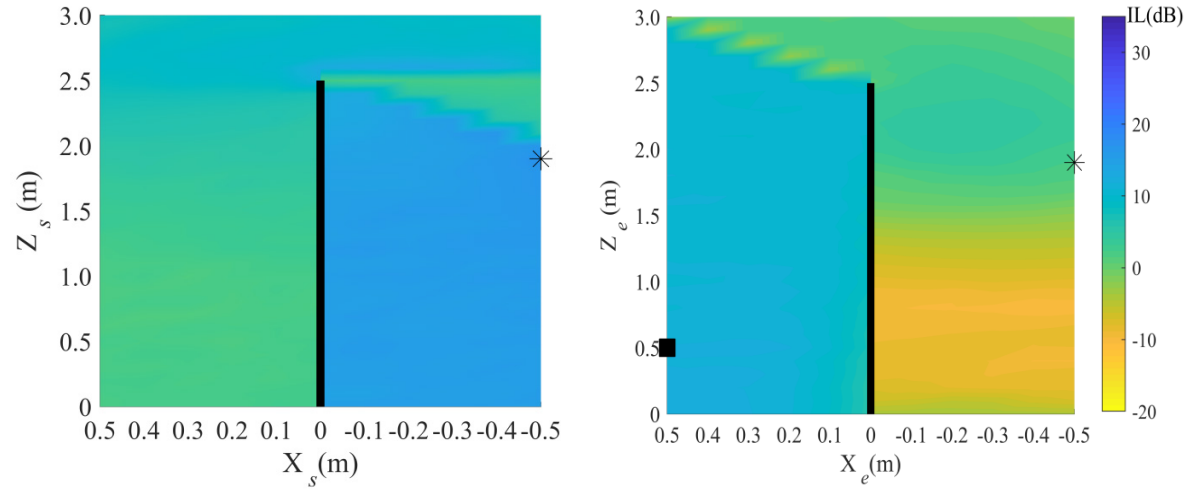

(**b-i**) (**b-ii**)

Figure 5. *Cont.*

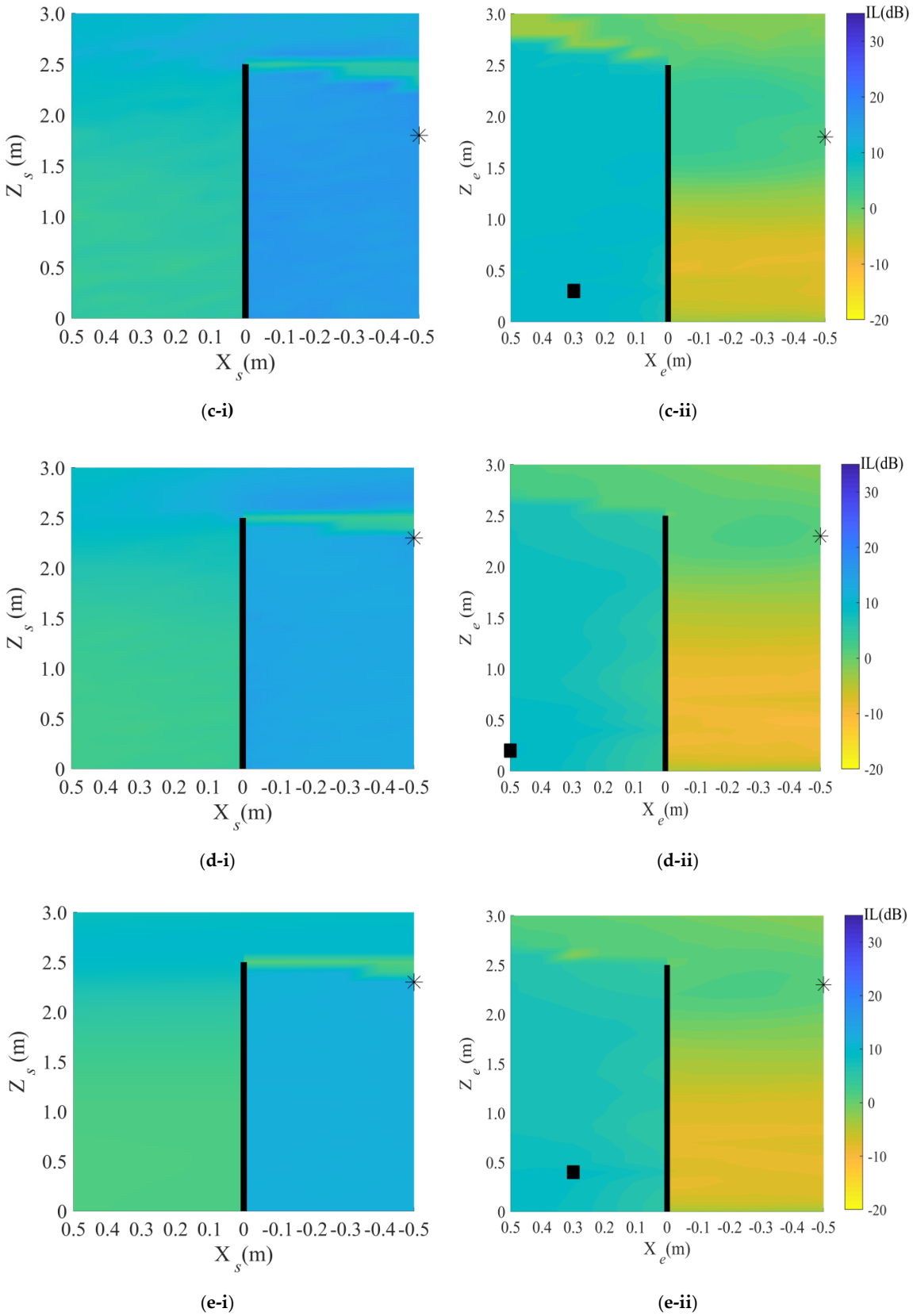

Figure 5. $\overline{IL}_{FS}$ (dB) for different positions of (**i**) secondary sources and (**ii**) error microphones in the control zone. The distance of the noise source (d_{pr}) is (**a**) 1 m, (**b**) 2.5 m, (**c**) 4 m, (**d**) 5.5 m, and (**e**) 7 m. * and ■ represent the best positions of the control sources and error microphones, respectively.

5. Discussion

5.1. Target Area: Street Area

Table 1 shows that the performances of both active and passive noise control mechanisms in the shadow zone of the barrier are of the same order for the range of distance of the noise source from the barrier (d_{pr}) studied in this investigation. It shows the farther the noise source from the barrier, the lower the attenuation achieved by both passive and active noise control mechanisms. The attenuation of active noise cancellation in the street area is in the range of 9.3 to 16.4 dB when the d_{pr} changes from 7 to 1 m, respectively. Passive attenuation, however, is more stable and varies from 11.4 to 14.9 dB for the same distances of the noise source. The loss of attenuation with the active mechanism is not very noticeable for d_{pr} more than 2.5 m. The same results were observed for the attenuation attained in the shadow zone of the façade. These observations imply that the active cancellation is more sensitive than passive noise control to the changes in the distance of the noise from the barrier.

Table 1 also shows when the target zone is the street area, the active noise barrier can reduce the noise level at the shadow zone of the façade, but it fails to achieve reductions in the whole façade for d_{pr} from 4 to 7 m. The possible explanation for this result is the noise source farther from 4 m, the number of observational points on the top parts of the façade, which receive direct wave fronts of the noise source, and diffracted wave fronts from the control sources increase, and the control source diffracted field cannot reduce the direct field of the noise source. This suggests that the noise control mechanism is to cancel the diffracted wave fronts rather than the primary noise radiation.

Moreover, the positions for the control sources and error sensors show that they are always located on the incident side and shadow side of the barrier, respectively. However, the locations are different for each position of the noise source, and for a practical active noise barrier in a changing environment such as a construction site, it is mandatory to seek a unique configuration for the whole range of the noise source's position.

Figure 4 reveals that the position of the control sources and the error microphones significantly contributes to the performance of the control system. Figure 4-i shows that when the squared pressures are minimized directly at the observational points in the street area, there is a rather wide suitable region in the incident side of the control zone for the control sources to be located. However, there is a narrow region in the incident side of the barrier where the control sources achieve lower attenuation in the street area (Figure 4-i). When the control sources are placed in this narrow region, some observational points receive both direct and diffracted wave fronts, while other observational points just receive diffracted wave fronts. This mixture of control sources' field in the target area likely explains the weak performance of the control system for noise control, as it is shown for example in the work of Chen et al. [18] where the active cancellation of the barrier is basically achieved in the region of diffracted primary sound field. Thus, taking into account the position of the street area, the suitable region for the secondary sources is a relatively broad region below the edge of the barrier at the incident side.

Figure 4-ii displays that the active noise barrier is more efficient for those positions of the error sensors in the control zone where they receive the same wave-fronts from the noise source and secondary sources as the target area. Considering the best positions of the control sources presented in Table 1, the suitable region for the error sensors is the shadow side of the barrier and below the noise source-edge line.

There is no prior study that considered a whole range of positions for transducers around the barrier, but some previous studies confirm the results of the current investigation. Omoto et al. [24] and Fan et al. [44] showed that for both straight and T-shaped active noise barriers, the better performance achieves when the control sources are placed in the incident side of the barrier, along the line that connects the noise source to the edge of the barrier.

5.2. Target Area: Shadow Zone of the Façade

The same method is used to define the suitable regions of the transducers when the target area is the shadow zone on the façade. As shown in Table 2, the optimal positions for the secondary sources

are in the noise source incident side and the error sensors are in the shadow side. This table also illustrates that when the shadow zone on the façade of the building is considered as the target area, the active noise control is as effective as the passive noise barrier to reduce the noise level. The trend of insertion loss is rather similar to the results obtained when the street area was considered as the target area.

Generally speaking, Figure 5 demonstrates that the suitable regions for the control sources and error sensors are below the line that connects the noise source to the barrier edge at the incident and at the shadow side, respectively. These regions closely match the locations previously proposed for the street area. Locating the transducers above this line adversely affects the performance of the active noise barrier. Results of ref. [45] also confirm that the error microphones placed in the shadow zone of the barrier could create a large quiet zone in the shadow area.

Comparing the reductions achieved for these two target areas presented in Tables 1 and 2 and Figure 4-ii and Figure 5-ii propose a unique configuration for the positions of the control means.

Figure 6a,b illustrates the insertion loss in the street area when the noise source is at $d_{pr} = 7$ m and the transducers are located in the positions presented in Tables 1 and 2, respectively. This figure shows approximately the same noise level reduction in the street area regardless of the location of the control zones. On the other hand, Figure 7 shows the insertion loss (dB) in the shadow zone of the façade for the same condition. This figure reveals that the active noise barrier achieves more reduction on the building façade when this area is considered as the control zone. Comparing these two figures reveals that the active noise barrier achieves better noise reduction in both areas when the shadow zone on the façade is considered as the target area.

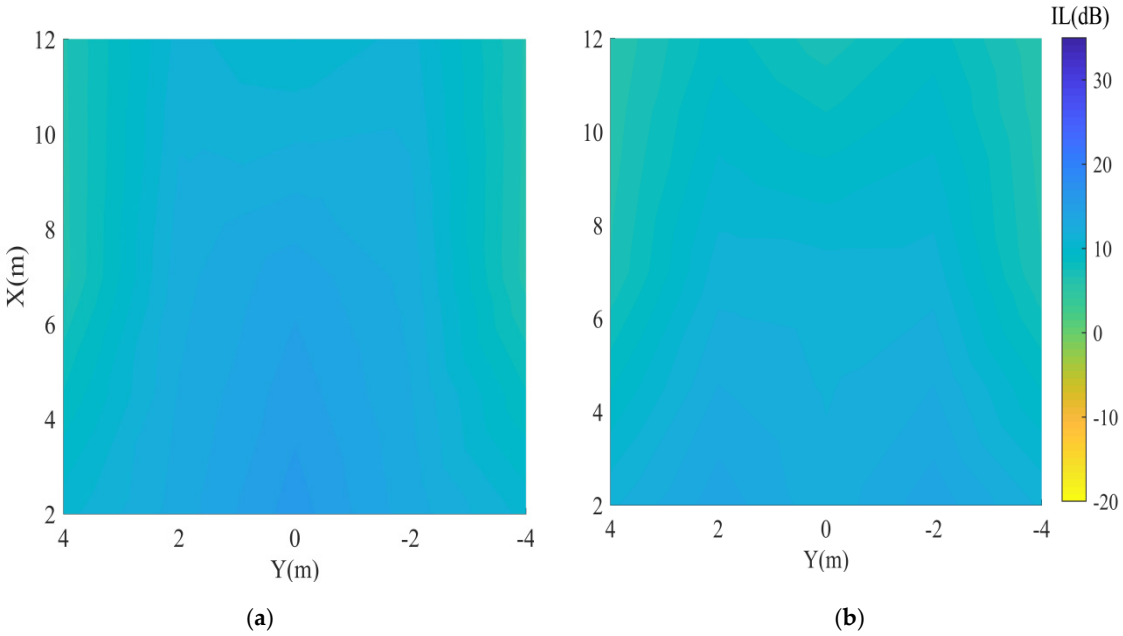

Figure 6. Insertion loss (dB) in the street area when the noise source is at $d_{pr} = 7$ m and the control zone is (**a**) the street area ((X_s, Z_s) = (−0.5, 1.8), (X_e, Z_e) = (0.4,0.2)) and (**b**) the shadow zone on the façade ((X_s, Z_s) = (−0.5, 2.3), (X_e, Z_e) = (0.3,0.4)).

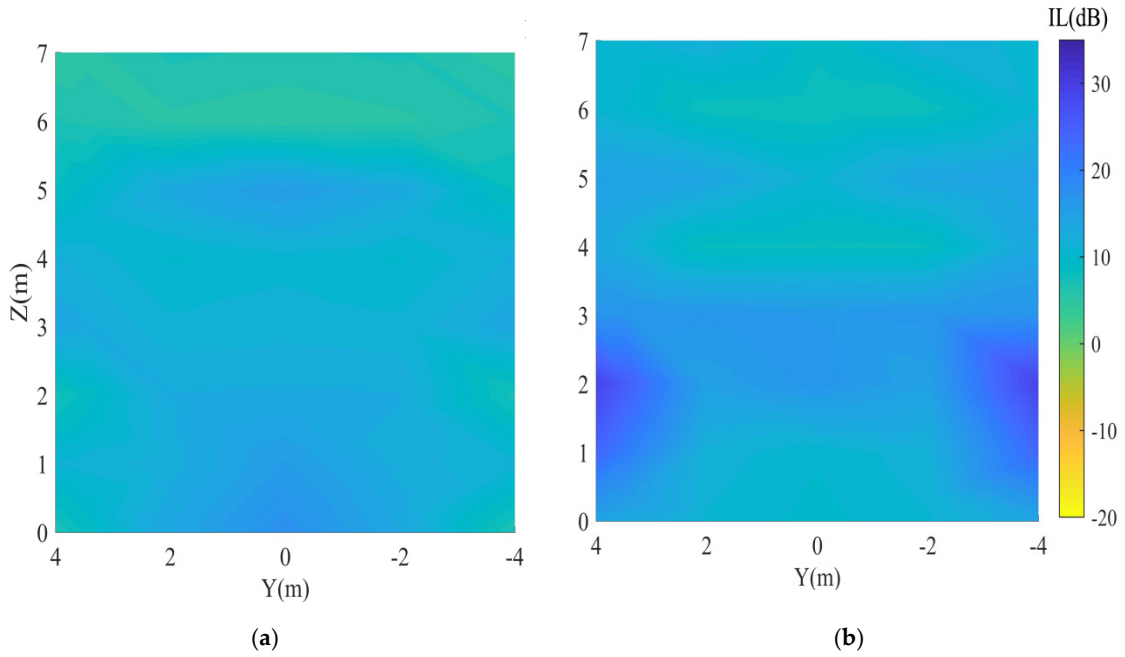

Figure 7. Insertion loss at the observational points in the shadow zone of façade, $\overline{IL}_{FS}$ (dB), when (**a**) street area ((X_s, Z_s) = (−0.5, 1.8), (X_e, Z_e)= (0.4,0.2)) and (**b**) shadow zone on the façade((X_s, Z_s) = (−0.5, 2.3), (X_e, Z_e) = (0.3,0.4)) are the target areas.

6. Conclusions

Successful implementation of an active noise barrier close to a construction site requires an effective configuration for the control devices and a good understanding of different scenarios for a moving noise source. The main contribution of this work is studying the suitability of an active noise barrier to control the construction noise activities in the neighboring street area and the nearby building façade for a noise source in the construction site. The noise source is represented by a point source placed at different positions regarding the barrier (as a mobile source would do) and operates with the typical sound spectra of construction noises.

Although a single optimal configuration is found that gives the maximum attenuation for any plant configuration, results suggest that there is a suitable broad region for locating the transducers with quite similar results of attenuation for most of the different plant conditions (in this study, the distance between the noise source and the barrier and the position of the cancellation target zone). The suitable region for the control sources is whatever position below the line that connects the noise source to the edge of the barrier and as far as possible from the barrier (0.5 m in this study). The region for the error sensors also is whatever position in the diffracted field of the shadow zone and as possible from the barrier (0.5 m in this study), which is below the line between the edge of the barrier and the farthest receiver.

Whatever configuration that follows these rules and for the number of sources and error sensors considered in this study, good attenuation results are yielded in the whole shadow zone behind the array of the error sensors, as cancellation at any of the two target areas has always achieved good attenuation in the other zones. It is shown that with the geometry of this study for the target zones, when the noise source is 7 m far away from the barrier, the passive attenuation of the barrier reduces the noise level to 11.4 and 9.1 dB in the street area and in shadow zone of the façade, respectively. Besides, the active cancellation with the optimized configuration for the control transducers when the shadow zone of the façade is the target area can increase the noise mitigation level to 20.3 and 17.4 dB in the street area and the shadow zone of the façade, respectively. An implication of these results is the expandability of the implementation of the active noise barrier to control broad cases of construction noise scenarios.

As an additional criterion, the barrier should be placed as close as possible to the noise source, to reduce the risk of raising the noise level in the top part of the building. However, the overall performance of the proposed configuration is also relatively independent of the position of the noise source, as the attenuation in the shadow zone of the barrier remains almost unchanged for distances between the noise source and the barrier between 2.5 and 7 m.

Author Contributions: Conceptualization, S.S., T.P.G. and J.R.G.; methodology, S.S., T.P.G. and J.R.G.; code developing, S.S.; formal analysis, S.S., T.P.G. and J.R.G.; investigation, S.S., T.P.G. and J.R.G.; writing—original draft preparation, S.S.; writing—review and editing, T.P.G. and J.R.G.; visualization, S.S.; supervision, T.P.G. and J.R.G. All authors have read and agreed to the published version of the manuscript.

Funding: This research was funded by a grant from Agència de Gestió d'Ajuts Universitaris i de Recerca, grant number is 2020 FI_B2 00073.

Acknowledgments: This research was financially supported by Agència de Gestió d'Ajuts Universitaris i de Recerca (AGAUR) from Generalitat de Catalunya. Shahin Sohrabi. would like to express his gratitude to the AGAUR for financial support. The authors would like to thank the reviewers for their constructive feedback.

Conflicts of Interest: The authors declare no conflict of interest.

References

1. Lee, S.C.; Kim, J.H.; Hong, J.Y. Characterizing perceived aspects of adverse impact of noise on construction managers on construction sites. *Build. Environ.* **2019**, *152*, 17–27. [CrossRef]
2. Li, X.; Song, Z.; Wang, T.; Zheng, Y.; Ning, X. Health impacts of construction noise on workers: A quantitative assessment model based on exposure measurement. *J. Clean. Prod.* **2016**, *135*, 721–731. [CrossRef]
3. Lee, S.C.; Hong, J.Y.; Jeon, J.Y. Effects of acoustic characteristics of combined construction noise on annoyance. *Build. Environ.* **2015**, *92*, 657–667. [CrossRef]
4. Liu, Y.; Xia, B.; Cui, C.; Skitmore, M. Community response to construction noise in three central cities of Zhejiang province, China. *Environ. Pollut.* **2017**, *230*, 1009–1017. [CrossRef] [PubMed]
5. Kwon, N.; Song, K.; Lee, H.-S.; Kim, J.; Park, M. Construction Noise Risk Assessment Model Focusing on Construction Equipment. *J. Constr. Eng. Manag.* **2018**, *144*, 1–12. [CrossRef]
6. Ng, C.F. Effects of building construction noise on residents: A quasi-experiment. *J. Environ. Psychol.* **2000**, *20*, 375–385. [CrossRef]
7. Ballesteros, M.J.; Fernandez, M.D.; Quintana, S.; Ballesteros, J.A.; González, I. Noise emission evolution on construction sites. Measurement for controlling and assessing its impact on the people and on the environment. *Build. Environ.* **2010**, *45*, 711–717. [CrossRef]
8. Cheng, K.W.; Law, C.W.; Wong, C.L. Quiet construction: State-of-the-art methods and mitigation measures. In Proceedings of the Internoise 2014—43rd International Congress on Noise Control Engineering, Melbourne, Australian, 16–19 November 2014; pp. 1–10.
9. Kwon, N.; Park, M.; Lee, H.-S.; Ahn, J.; Shin, M. Construction Noise Management Using Active Noise Control Techniques. *J. Constr. Eng. Manag.* **2016**, *142*. [CrossRef]
10. Gilchrist, A.; Allouche, E.N.; Cowan, D. Prediction and mitigation of construction noise in an urban environment. *Can. J. Civ. Eng.* **2003**, *30*, 659–672. [CrossRef]
11. Thalheimer, E. Construction noise control program and mitigation strategy at the Central Artery/Tunnel Project. *Noise Control. Eng. J.* **2000**, *48*, 157. [CrossRef]
12. Zhaomeng, W.; Meng, L.K.; Priyadarshinee, P.; Pueh, L.H. Applications of noise barriers with a slanted flat-tip jagged cantilever for noise attenuation on a construction site. *J. Vib. Control.* **2017**, *24*, 5225–5232. [CrossRef]
13. Ireland, T.I.; Centre, P.B.; Street, P. Noise management during the construction of a light rail scheme through Dublin city centre. In Proceedings of the INTER-NOISE 2019, Madrid, Spain, 16–19 June 2019.
14. Wilson, P.M. Innovations that make infrastructure and construction noise control more effective. In Proceedings of the INTER-NOISE 2016—45th International Congress and Exposition on Noise Control Engineering, Hamburg, Germany, 21–24 August 2016.
15. Lee, H.P.; Tan, L.B.; Lim, K.M. Assessment of the performance of sonic crystal noise barriers for the mitigation of construction noise. In Proceedings of the INTER-NOISE 2016—45th International Congress and Exposition on Noise Control Engineering, Hamburg, Germany, 21–24 August 2016; pp. 4220–4226.

16. Lee, H.M.; Wang, Z.; Lim, K.M.; Lee, H.P. A Review of Active Noise Control Applications on Noise Barrier in Three-Dimensional/Open Space: Myths and Challenges. *Fluct. Noise Lett.* **2019**, *18*, 1–21. [CrossRef]
17. Kanazawa, L.; Mizutani, K. Reduction of construction machinery noise in multiple dominant frequencies using feedforward type active control. In Proceedings of the INTER-NOISE 2018—47th International Congress and Exposition on Noise Control Engineering, Chicago, IL, USA, 26–29 August 2018.
18. Chen, W.; Min, H.; Qiu, X. Noise reduction mechanisms of active noise barriers. *Noise Control Eng. J.* **2013**, *61*, 120–126.
19. Han, N.; Qiu, X. A study of sound intensity control for active noise barriers. *Phys. Appl. Acoust.* **2007**, *68*, 1297–1306. [CrossRef]
20. Guo, J.; Pan, J. Increasing the insertion loss of noise barriers using an active-control system. *J. Acoust. Soc. Am.* **1998**, *104*, 3408–3416. [CrossRef]
21. Omoto, A. Active suppression of sound diffracted by a barrier: An outdoor experiment. *J. Acoust. Soc. Am.* **1997**, *102*, 1671–1679. [CrossRef]
22. Rubio, C.; Castiñeira-Ibañez, S.; Uris, A.; Belmar, F.; Candelas, P. Numerical simulation and laboratory measurements on an open tunable acoustic barrier. *Appl. Acoust.* **2018**, *141*, 144–150. [CrossRef]
23. Reiter, P.; Wehr, R.; Ziegelwanger, H. Simulation and measurement of noise barrier sound-reflection properties. *Appl. Acoust.* **2017**, *123*, 133–142. [CrossRef]
24. Omoto, A. A study of an actively controlled noise barrier. *J. Acoust. Soc. Am.* **1993**, *94*, 2173. [CrossRef]
25. Niu, F.; Zou, H.; Qiu, X.; Wu, M. Error sensor location optimization for active soft edge noise barrier. *J. Sound Vib.* **2007**, *299*, 409–417. [CrossRef]
26. Liu, J.C.; Niu, F. Study on the analogy feedback active soft edge noise barrier. *Appl. Acoust.* **2008**, *69*, 728–732. [CrossRef]
27. Hart, C.R.; Lau, S.-K. Active noise control with linear control source and sensor arrays for a noise barrier. *J. Sound Vib.* **2012**, *331*, 15–26. [CrossRef]
28. Chen, W.; Rao, W.; Min, H.; Qiu, X. An active noise barrier with unidirectional secondary sources. *Appl. Acoust.* **2011**, *72*, 969–974. [CrossRef]
29. Duhamel, D.; Sergent, P.; Hua, C.; Cintra, D. Measurement of active control efficiency around noise barriers. *Appl. Acoust.* **1998**, *55*, 217–241. [CrossRef]
30. Li, K.; Wong, H. A review of commonly used analytical and empirical formulae for predicting sound diffracted by a thin screen. *Appl. Acoust.* **2005**, *66*, 45–76. [CrossRef]
31. Ohnishi, K.; Saito, T.; Teranishi, S.; Namikawa, Y.; Mori, T.; Kimura, K.; Uesaka, K. Development of the product-type active soft edge noise barrier. In Proceedings of the 18th International Congress on Acoustics, Kyoto, Japan, 4–9 April 2004; pp. 1041–1044.
32. Berkhoff, A.P. Control strategies for active noise barriers using near-field error sensing. *J. Acoust. Soc. Am.* **2005**, *118*, 1469–1479. [CrossRef]
33. Guo, J.; Pan, J. Application of active noise control to noise barriers. *Acoust. Aust.* **1997**, *25*, 11–16.
34. Lau, S.-K.; Tang, S.K. Sound fields in a rectangular enclosure under active sound transmission control. *J. Acoust. Soc. Am.* **2001**, *110*, 925–938. [CrossRef]
35. Palacios, J.I.; Romeu, J.; Balastegui, A. Two Step Optimization of Transducer Locations in Single Input Single Output Tonal Global Active Noise Control in Enclosures. *J. Vib. Acoust.* **2010**, *132*, 061011. [CrossRef]
36. Monson, B.B.; Sommerfeldt, S.D.; Gee, K.L. Improving compactness for active noise control of a small axial cooling fan. *Noise Control. Eng. J.* **2007**, *55*, 397. [CrossRef]
37. Martin, V.; Gronier, C. Sensor configuration efficiency and robustness against spatial error in the primary field for active sound control. *J. Sound Vib.* **2001**, *246*, 679–704. [CrossRef]
38. Romeu, J.; Palacios, J.I.; Balastegui, A.; Pàmies, T. Optimization of the Active Control of Turboprop Cabin Noise. *J. Aircr.* **2015**, *52*, 1386–1393. [CrossRef]
39. Sjösten, P.; Johansson, S.; Persson, P.; Claesson, I. Considerations on Large Applications of Active Noise Control. Part II: Experimental Results. *Acta Acust.* **2003**, *89*, 834–843.
40. Macdonald, H.M. A Class of Diffraction Problems. *Proc. Lond. Math. Soc.* **1915**. [CrossRef]
41. Elliott, S.; Nelson, P. The active control of sound. *Electron. Commun. Eng. J.* **1990**, *2*, 127–136. [CrossRef]
42. Matsui, T.; Takagi, K.; Hiramatsu, K.; Yamamoto, T. Outdoor sound propagation from a source having dimensions. *J. Acoust. Soc. Jpn.* **1989**. [CrossRef]

43. Shao, J.; Sha, J.-Z.; Zhang, Z.-L. The method of the minimum sum of squared acoustic pressures in an actively controlled noise barrier. *J. Sound Vib.* **1997**, *204*, 381–385. [CrossRef]
44. Fan, R.; Su, Z.; Cheng, L. Modeling, analysis, and validation of an active T-shaped noise barrier. *J. Acoust. Soc. Am.* **2013**, *134*, 1990–2003. [CrossRef]
45. Ise, S.; Yano, H.; Tachibana, H. Basic study on active noise barrier. *J. Acoust. Soc. Jpn.* **1991**, *12*, 299–306. [CrossRef]